Journal of Alloys and Compounds 489 (2010) 310–315

Contents lists available at ScienceDirect

Journal of Alloys and Compounds

journal homepage: www.elsevier.com/locate/jallcom

Studies on magnetic, dielectric and magnetoelectric behavior of (x) $NiFe_{1.9}Mn_{0.1}O_4$ and $(1-x)$ $BaZr_{0.08}Ti_{0.92}O_3$ magnetoelectric composites

R.C. Kambale[a], P.A. Shaikh[a], C.H. Bhosale[a], K.Y. Rajpure[a], Y.D. Kolekar[b,*]

[a] Composite Materials Laboratory, Department of Physics, Shivaji University, Kolhapur 416004 (M.S.), India
[b] Department of Physics, University of Pune, Ganeshkhind, Pune 411007 (M.S.), India

ARTICLE INFO

Article history:
Received 7 August 2009
Received in revised form
14 September 2009
Accepted 15 September 2009
Available online 23 September 2009

Keywords:
ME composites
X-ray diffraction
Dielectric properties
Ferroelectricity
Magnetic properties

ABSTRACT

In the present research work, the magnetoelectric (ME) composites of ferrite and ferroelectric phases with (x) $NiFe_{1.9}Mn_{0.1}O_4$ and $(1-x)$ $BaZr_{0.08}Ti_{0.92}O_3$ (where $x = 0.10$, 0.20 and 0.30) respectively were synthesized by the conventional ceramic method. The X-ray diffraction pattern of the composite reveals a spinel phase formation for the ferrite and perovskite phase formation for the ferroelectric phase without any other phase. The SEM micrographs of composites were taken to determine the average grain size and also to study the surface morphology. The effect of constituent phase variation on the *B–H* hysteresis behavior and the dielectric properties was examined. The dielectric constant shows usual dielectric dispersion behavior with increasing frequency which is due to the Maxwell–Wagner type surface interfacial polarization. From the ac conductivity study, it is confirmed that the conduction in the present composites is of small polaron type. The static magnetoelectric (ME) voltage coefficient developed on the surface of magnetoelectric material was measured as a function of applied dc magnetic field. The maximum ME conversion factor of 1.18 mV/cm Oe was observed for $x = 0.10$ composite. Such composites may be useful to fabricate the magnetic field sensors and applicable in many linear ME devices.

1. Introduction

In recent years, the multiferroic materials [1–3] with coexistence of at least two ferroic orders (ferroelectric, ferromagnetic, or ferroelastic) have been drawn an increasing interest due to their potential applications as multifunctional devices. In multiferroic materials, the coupling interaction between the different order parameters could produce new effects, such as magnetoelectric (ME) effect [3–6]. The magnetoelectric response is the appearance of an electric polarization on the surface of the material upon applying a magnetic field and/or the appearance of a magnetization upon applying an electric field. Following figure shows the schematic representation of the ME effect [7] in the composites utilizing the product property [8].

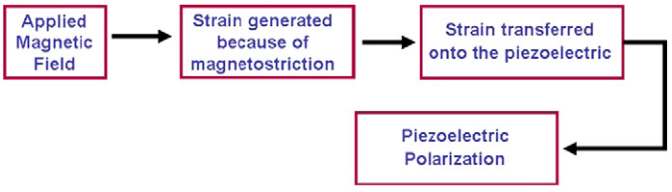

According to this principle, a suitable combination of two phases such as a combination of magnetostrictive (ferrite) and piezoelectric (ferroelectric) phases can yield a desirable ME property. The search for such systems was promoted by practical needs, due to the low ME voltage coefficient of the single-phase materials making them inadequate for practical applications and by the low temperature range for the ME effect, mostly at cryogenic temperatures [9]. The challenge in making such materials is to find equilibrium ferroelectric and magnetic structures preserving both properties close to the room temperature. The main advantages to prepare sintered ME composites are related to the easy and cheap fabrication and to the possibility to control the molar ratio of phases, grain size of each phase and densification [10]. In this paper we report the magnetic, dielectric and magnetoelectric sensing behavior of magnetoelectric (ME) composites in which the $BaZr_{0.08}Ti_{0.92}O_3$ (BZT8) is to be selected as a ferroelectric phase and $NiFe_{1.9}Mn_{0.1}O_4$ (NFM) as a ferrite phase. Recently, it has observed that the $BaZr_{0.08}Ti_{0.92}O_3$ has high dielectric permittivity and high piezoelectric coefficient [11]. While the $NiFe_{1.9}Mn_{0.1}O_4$ ferrite is selected because, the several reports states that the doping of Ni ferrite by other magnetic ions such as Mn, Co, Cu, etc. improves the resistivity, permeability, magnetization and coercive field of the nickel ferrite [12–14]. Van Uitert [15], reports that by incorporating small amounts of Mn(10%) to Fe in the nickel ferrite the resistivity of the nickel ferrite increases up to 10^{10} or 10^{11} Ω-cm. Therefore, by considering the Boomgaard's outline [16] to obtain good magnetoelectric response in ME com-

* Corresponding author.
E-mail addresses: rckambale@gmail.com (R.C. Kambale), ydkolekar@gmail.com (Y.D. Kolekar).

0925-8388/$ – see front matter © 2009 Elsevier B.V. All rights reserved.
doi:10.1016/j.jallcom.2009.09.080

posite the ferrite phase should have high resistivity. If, the ferrite phase has low resistivity then it leads to low ME output because low resistivity of the ferrite which limits the electric field used for poling the composite and consequently poor piezoelectric coupling and produces a leakage current in the loss of induced voltage.

2. Experimental procedure

2.1. Synthesis

Magnetoelectric composites (ME) of $NiFe_{1.9}Mn_{0.1}O_4$ and $BaZr_{0.08}Ti_{0.92}O_3$, i.e. (NFM-BZT) were prepared by the conventional ceramic method. The polycrystalline ferrite phase $NiFe_{1.9}Mn_{0.1}O_4$ (NFM) was prepared by using NiO, Fe_2O_3 and Mn_2O_3 as starting materials while the $BaZr_{0.08}Ti_{0.92}O_3$ (BZT8) ferroelectric phase was prepared from $BaCO_3$, ZrO_2 and TiO_2 as starting materials in appropriate molar proportions. The ferrite and ferroelectric phases were pre-sintered at 1000 °C and 1200 °C for 10 h and 2 h, respectively. The composites were prepared by mixing 10 mol%, 20 mol% and 30 mol% of the ferrite phase with 90 mol%, 80 mol% and 70 mol% of the ferroelectric phase, respectively. The mixed powders were uniaxially pressed into pellets (diameter = 15 mm and thickness ~1.2 mm) using a hydraulic press. The pelletized samples were then finally sintered at 1250 °C for 10 h and then used for various characterizations.

2.2. Characterization

X-ray diffraction (XRD; CuK_α radiation, model Bruker D8 Advance) was used for confirming the phase formation and structural study. The surface morphological features were observed by using scanning electron microscopy (SEM, model JSM-6360A). The ferromagnetic *B–H* hysteresis loop parameters such as saturation magnetization (*Ms*), retentivity (*Mr*) and coercive field (*Hc*) were measured from the observed *B–H* loop, recorded by using high field hysteresis loop tracer (Magneta, Mumbai) working on a 50 Hz mains frequency [17]. The magnetic moment n_B in Bohr magneton (μ_B) was calculated using the relation [18]:

$$n_B = \frac{M \times Ms}{5585} \quad (1)$$

where *M* is the molecular weight and *Ms* is the saturation magnetization per gram of the sample.

The dc resistivity was measured by the two probe method as a function of temperature (i.e., from room temperature to 550 °C.) The room temperature dielectric constant was measured by using a precision LCR meter bridge (model HP 4284 A) with frequency range from 20 Hz to 1 MHz, at room temperature. The ac conductivity was calculated from the dielectric data and using the following relation [19]:

$$\sigma_{ac} = 2\pi\varepsilon_0\varepsilon_r f \tan\delta \quad (2)$$

where σ_{ac} is ac conductivity of the sample, ε_0 is the permittivity of air, ε_r is the real part of dielectric constant of the sample, *f* is the frequency of the applied field, $\tan\delta$ is the loss factor. To improve the better ME signal, the samples have been poled electrically and magnetically. For electrical poling, the samples were heated to approximately 50 °C above the ferroelectric Curie temperature and then allowed to cool slowly in the presence of an electric field of about 2 kV cm^{-1}. A magnetic field of 4 kOe was applied across the sample in the direction of the electric field. The voltage developed on the surface of the samples, i.e. ME output was measured at room temperature by varying the applied dc magnetic field with the help of a Keithley electrometer (Model-6514).

3. Results and discussion

3.1. Phase identification

Fig. 1 shows X-ray diffraction (XRD) patterns of composite containing 10%, 20% and 30% ferrite phase, respectively. The results obtained from X-ray diffraction (XRD) study are in good agreement with the JCPDS card Nos. 74-2082, 83-1880 and 74-1299. All the diffraction peaks are characteristics of the constituent phases. It is well known that in the spinel cubic structure, i.e. ferrite, a (3 1 1) reflection is more intense, and in the tetragonal perovskite structures, i.e. ferroelectric, a (1 0 1) reflection is more intense. These two sets of well defined reflections are observed in the composite samples. No unidentified peaks are observed, suggesting that no chemical reactions have been occurred between the ferrite and ferroelectric phases during the final sintering. The observed structural parameters are listed in Table 1. The ferrite and ferroelectric phases, respectively, results into cubic spinel and tetragonal perovskite structures having the lattice parameters $a = 8.34$ Å and $a = 3.99$ Å, $c = 4.03$ Å ($c/a = 1.01$), respectively. The lattice parameters of the composites (Table 1) are almost equal to those of the constituent phases, indicating that no structural changes have been observed with the variation in mole percentages of the constituent phases and also during sintering process. The intensity and number of ferrite peaks should increase with the increase of ferrite content in the composites and the same trend is observed which is shown in Fig. 1.

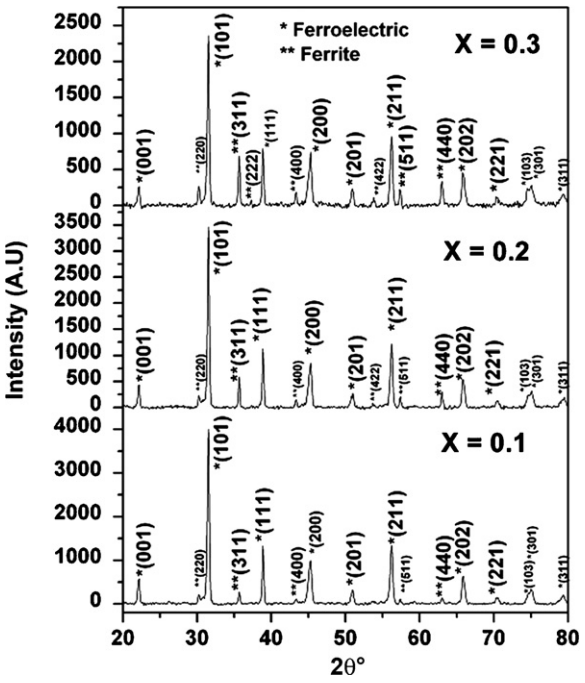

Fig. 1. X-ray diffraction patterns of (x) $NiFe_{1.9}Mn_{0.1}O_4 + (1-x)$ $BaZr_{0.08}Ti_{0.92}O_3$ ME composites.

Fig. 2 shows the series of scanning electron microscope (SEM) pictures of ferrite (NFM), ferroelectric (BZT8) and their ME composites with $x = 0.10$, 0.20 and 0.30, respectively. The average grain size was calculated by line intercept method and is listed in Table 1. The grain size is found to decrease with increase in ferrite content. In the present work average grain size for ferrite and ferroelectric phases was observed to be 0.50 μm and 0.83 μm, respectively. The grain size of the ferroelectric phase is larger than that of the ferrite phase. In the present investigation all the composites were prepared in a ferroelectric rich region, hence average grain size varies with the ferrite content. The average grain size for ME composites with $x = 0.10$, 0.20 and 0.30 are 0.33 μm, 0.25 μm and 0.20 μm, respectively. The decreased grain size results in a decrease of mean free path of the electrons and hence causes the change in resistivity [20].

3.2. Magnetic hysteresis

Figs. 3 and 4 show the *B–H* hysteresis loop of spinel ferrite phase and of composites with varying ferrite content respectively. At room temperature, all the samples exhibited *B–H* hysteresis loop typical of magnetic behavior, and this indicates that the presence of an ordered magnetic structure can exist in the mixed spinel–perovskite system. The *B–H* hysteresis loops of the composites shift towards the field axis with low ferrite content. All composites saturate at magnetic field strength of above ~1 kOe. The saturation magnetization (*Ms*) 46 emu/g was observed for the ferrite phase. Fig. 5 presents the variation of the theoretical and observed values of saturation magnetization as well as magnetic moment of the composites with varying ferrite content. From

Table 1
Structural, magnetic, resistivity and magnetoelectric data of $(x)\ NiFe_{1.9}Mn_{0.1}O_4 + (1-x)\ BaZr_{0.08}Ti_{0.92}O_3$ ME composites.

Composition(x)	Lattice parameters (Å)			Average grain size (μm)	Ms (emu/g)	μ_B	Mr (emu/g)	Resistivity at R.T. (Ω-cm)	Activation energy (eV)	$(dE/dH)_H$ (mV/cm Oe)
	Ferrite	Ferroelectric	c/a							
0.0	–	$a = 3.99$ $c = 4.03$	1.01	0.83	–	–	–	$\sim 10^{12}$	0.38	–
0.1	8.34	$a = 3.99$ $c = 4.03$	1.01	0.33	3.38	0.14	1.0	$\sim 10^{11}$	0.33	1.18
0.2	8.34	$a = 3.99$ $c = 4.03$	1.01	0.25	6.66	0.28	2.80	$\sim 10^{10}$	0.26	0.88
0.3	8.34	$a = 3.99$ $c = 4.03$	1.01	0.20	13.38	0.56	4.50	$\sim 10^{9}$	0.22	0.68
1.0	8.34	–		0.50	46.00	1.92	9.65	$\sim 10^{8}$	0.20	–

Table 1, it is observed that in composites the magnetic parameters like saturation magnetization *Ms*, magnetic moment n_B Bohr magneton and retentivity *Mr* increases as ferrite content increases. This is due to the individual grains of ferrite contributing to magnetization. The presence of pores among the grains breaks the magnetic circuits and results in a reduction of magnetic properties with increasing pore concentration [21]. Therefore, in composites, ferroelectric material in the presence of magnetic field acts as a pore causing the reduction of magnetic parameters. After saturation of a ferrite phase in a strong magnetic field, the magnetization vector rotates towards the nearest preferred field direction and results in high anisotropy when the field is reduced to zero. The

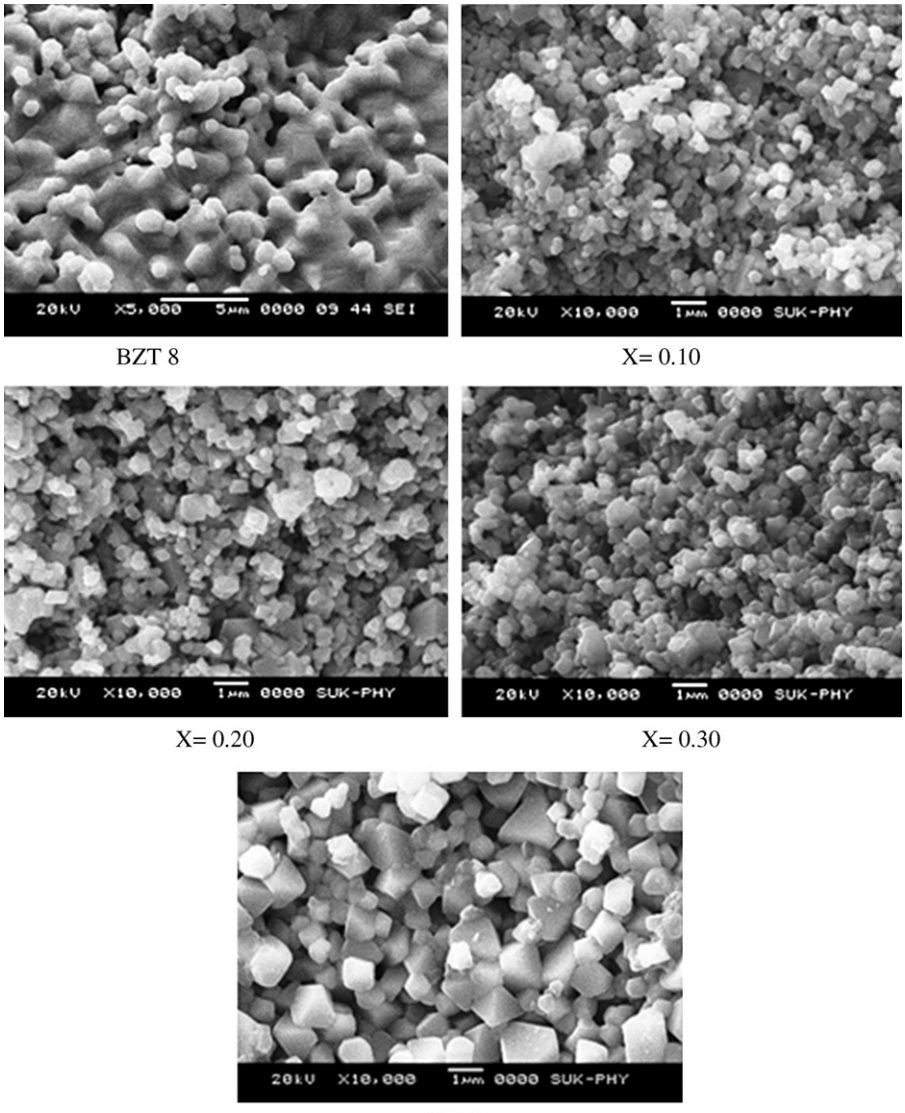

Fig. 2. SEM micrographs for $(x)\ NiFe_{1.9}Mn_{0.1}O_4 + (1-x)\ BaZr_{0.08}Ti_{0.92}O_3$ ME composites.

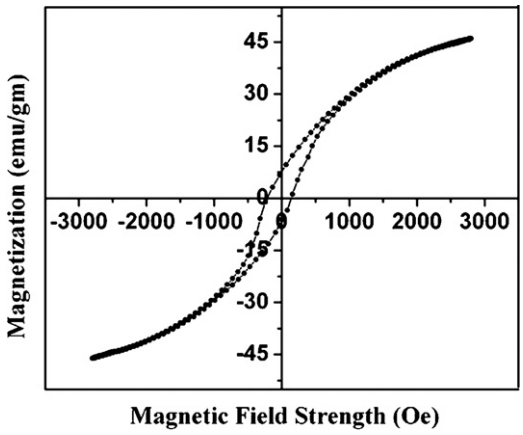

Fig. 3. *B–H* hysteresis loop of $NiFe_{1.9}Mn_{0.1}O_4$ ferrite phase.

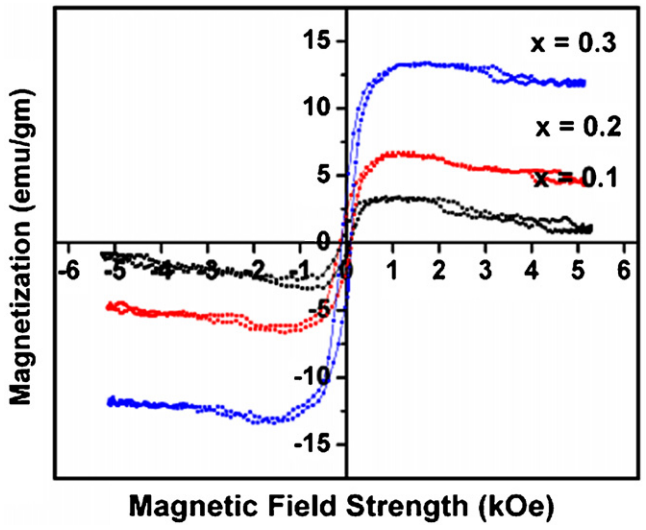

Fig. 4. *B–H* hysteresis loops for $(x)\,NiFe_{1.9}Mn_{0.1}O_4 + (1-x)\,BaZr_{0.08}Ti_{0.92}O_3$ ME composites.

stress and shape anisotropy are the most important parameters for getting the maximum magnetoelectric output in such composites. The increased values of retentivity suggests that most of the magnetization vectors are turned out of the magnetically preferred direction by making a small angle with the direction

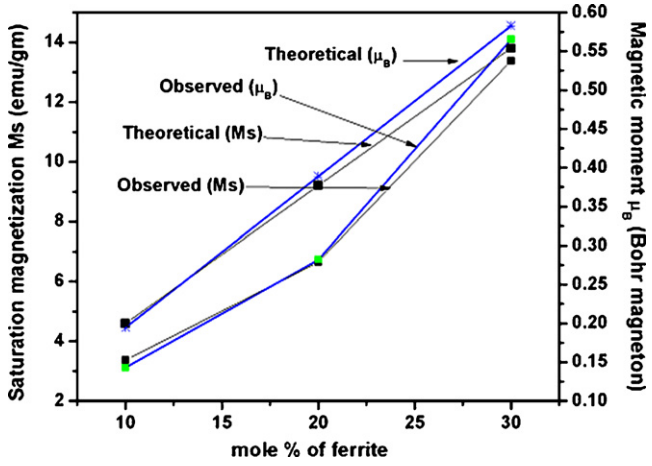

Fig. 5. Variation of saturation magnetization and magnetic moment in composites with ferrite content.

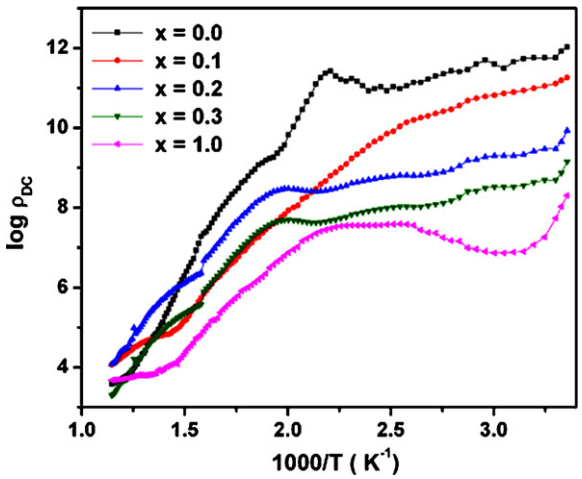

Fig. 6. Variation of DC resistivity with temperature for $(x)\,NiFe_{1.9}Mn_{0.1}O_4 + (1-x)\,BaZr_{0.08}Ti_{0.92}O_3$ ME composites.

of the applied field and suffer stresses [22], which result in high magnetization.

3.3. Electrical properties

The temperature dependence of dc resistivity is shown in Fig. 6. Linear decrease in resistivity with temperature reflects the semiconductor behavior of the samples. The decrease in resistivity with increase in temperature is due to increase in the thermally activated drift mobility of charge carriers according to the hopping conduction mechanism [20]. Also the resistivity of ME composites is fond to decrease with increase in ferrite content, this is because when the ferrite particles make chains, the electric resistivity of the composites is reduced significantly because of the low resistivity of the ferrite phase [23] as well as to the parallel connectivity between the ferrite and ferroelectric grains in all composites [24].

The activation energy was calculated by using the relation;

$$\rho = \rho_0 \exp\left(\frac{\Delta E}{kT}\right) \tag{3}$$

where ΔE is the activation energy, ρ is resistivity at room temperature, k is Boltzmann constant and ρ_0 is temperature independent constant. The resistivity and activation energy for ME composites are given in Table 1.It is well known that the electron and hole hopping between Fe^{2+}/Fe^{3+}, Ni^{2+}/Ni^{3+}, Mn^{2+}/Mn^{3+}, Ba^{2+}/Ba^{3+}, Ti^{3+}/Ti^{4+} and Zr^{3+}/Zr^{4+} ions, with activation energy <0.2 eV is responsible for electrical conduction in the composites. The calculated activation energies are 0.38 eV, 0.33 eV, 0.26 eV, 0.22 eV and 0.20 eV (in higher temperature region) for the composite with $x = 0$, 0.1, 0.2, 0.3 and 1, respectively, suggesting the temperature dependence of charge mobility.

Fig. 7 shows the frequency dependence of the dielectric constant of constituent phases as well as their composites. The $BaZr_{0.08}Ti_{0.92}O_3$ is a good dielectric material having dielectric constant larger than that of $NiFe_{1.9}Mn_{0.1}O_4$ ferrite. It was observed that the dielectric constant decreases steeply at lower frequencies and remains constant at higher frequencies indicating the usual dielectric dispersion. This may be attributed to the dipoles resulting from changes in valence states of cations and space charge polarization. At higher frequencies, the dielectric constant remains independent of frequency due to inability of electric dipoles to follow the alternating applied electric field [25]. These frequency independent values are known as static values of the dielectric constant. The higher dielectric constant at lower frequencies is associated

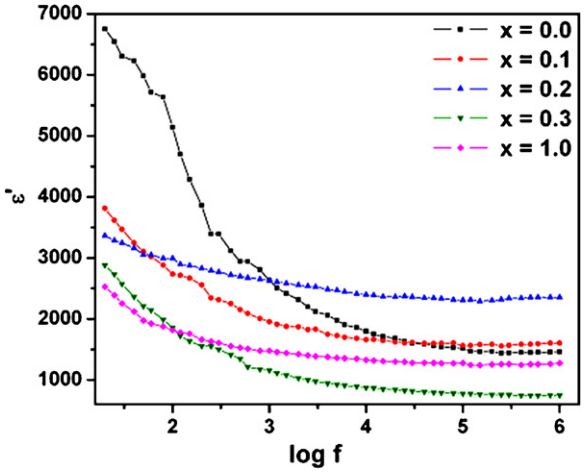

Fig. 7. Variation of dielectric constant with frequency for $(x)\,NiFe_{1.9}Mn_{0.1}O_4 + (1-x)\,BaZr_{0.08}Ti_{0.92}O_3$ ME composites.

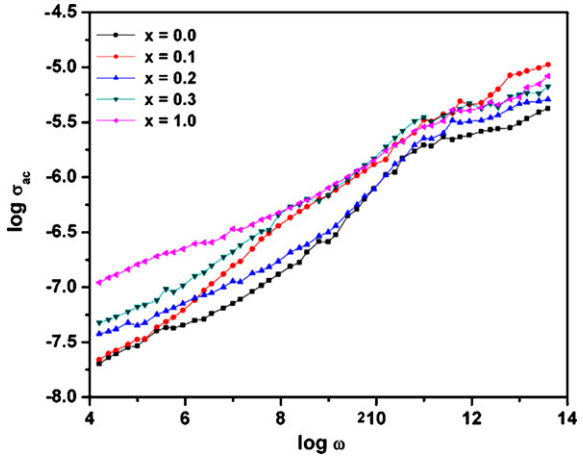

Fig. 8. Plots for ac conductivity of $(x)\,NiFe_{1.9}Mn_{0.1}O_4 + (1-x)\,BaZr_{0.08}Ti_{0.92}O_3$ ME composites.

with heterogeneous conduction in composites [26], but sometimes the polaron hopping mechanism results in electronic polarization contributing to low frequency dispersion. This is also attributed to Maxwell–Wagner [27,28] type interfacial polarization in agreement with the Koop's theory [29]. The dielectric behavior in the composites can also be explained on the basis of polarization mechanism in ferrite, which is similar to the conduction process because conduction in composites beyond phase percolation limits is due to the ferrite phase [30]. The existence of Fe^{3+}/Fe^{2+} ions has rendered ferrite materials dipolar. Since in ferrite, the rotation of $Fe^{2+} \leftrightarrow Fe^{3+}$ dipoles results in orientational polarization that may be visualized as an exchange of electrons between the ions, the dipoles align themselves with the alternating field. The constant values of ε_r at higher frequencies may be attributed to the fact that beyond a certain fixed frequency, the electron exchange between $Fe^{2+} \leftrightarrow Fe^{3+}$ does not follow the alternating field. In the present ferrite, the presence of Ni^{2+}/Ni^{3+} and Mn^{2+}/Mn^{3+} ions give rise to p-type carriers and their displacement in an external electric field direction contributes to the net polarization in additional n-type carriers. However, the p-type carrier contribution is smaller than that from the electronic exchange between ions and opposite in sign [31]. The electrical conductivity and dielectric dispersion of ferrites are mainly due to the exchange mechanism of charge carriers among the ions situated at crystallographically equivalent sites [32]. The dielectric constant is roughly inversely proportional to the square root of resistivity and same behavior is observed in the present study.

3.4. Ac conductivity

In order to understand the conduction mechanism and the type of polarons responsible for conduction ac conductivity measurements were carried out at room temperature in the frequency range from 20 Hz to 1 MHz. It is well known that in large polaron hopping the ac conductivity decreases with frequency and in small polaron hopping conductivity increases with frequency [17,24,33]. Fig. 8 shows the frequency-dependent ac conductivity plot. From this figure, the conductivity is observed to increase with an increase in frequency for all the composites. Linear variation of ac conductivity indicates that the conduction occurs by the hopping of charge carriers between localized states .The results are similar to the one observed by other workers [34,35]. For the present composites plots are linear confirming small polaron type of conduction. It has been shown that for ionic solids the concept of small polaron is valid [36]. The frequency-dependent conduction may be attributed to small polarons, as reported by Alder and Fienleib [37]. Hence the present results indicate that the conduction is due to small polarons in the composite which is responsible for the good ME response.

3.5. Magnetoelectric effect

The variation of ME output, $(dE/dH)_H$, as a function of magnetic field, H, is shown in Fig. 9. From this figure, it is observed that $(dE/dH)_H$ initially increases up to a certain magnetic field and finally attains a maximum value and then decreases with an increase in applied dc magnetic field. This is because in the spinel ferrite the magnetostrictive coefficient reaches to saturation at a certain value of magnetic field. Beyond saturation the magnetostriction and the strain thus produced would also produce a constant electric field in the piezoelectric phase making the $(dE/dH)_H$ decrease with the increasing magnetic field [38].

Also, the effect of grain size on piezoelectric, dielectric, and ferroelectric properties has been widely studied for ME composites in the literature [39–41] and it was found that grain size has significant effect on the piezoelectric, ferroelectric, and dielectric properties of the composite and hence influences the ME property. Fig. 10 shows the variation of ME voltage coefficient and dc resistivity with mol% of ferrite content. The magnetoelectric voltage coefficient $(dE/dH)_H$ decreases with an increase of ferrite content in the composites.

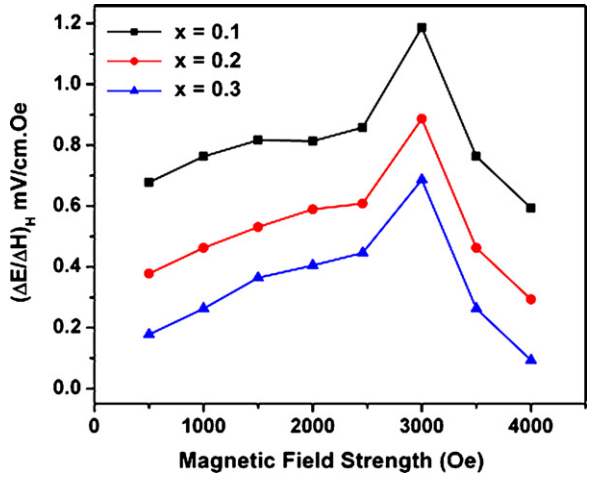

Fig. 9. Variation of ME response of $(x)\,NiFe_{1.9}Mn_{0.1}O_4 + (1-x)\,BaZr_{0.08}Ti_{0.92}O_3$ ME composites.

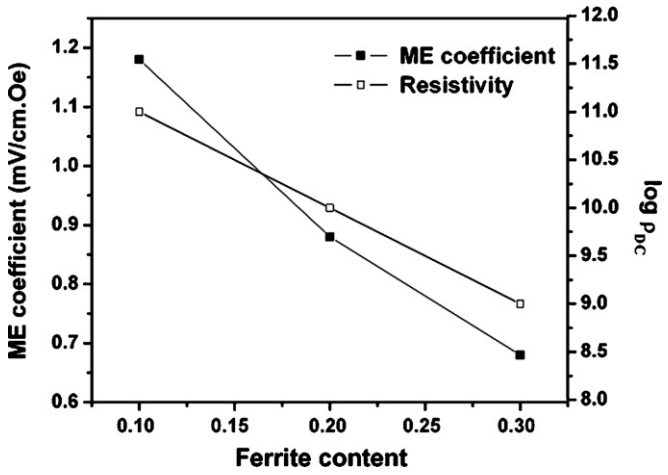

Fig. 10. Variation of ME voltage coefficient and dc resistivity with mol% of ferrite content.

In the present case maximum value of the ME voltage coefficient (1.18 mV/cm Oe) and dc resistivity ($\sim 10^{11}$ Ωcm) are observed for the composite with x = 0.10 than x = 0.20 and 0.30. This is because the grain size of the composites decreases with the addition of ferrite content which affect on the resistivity of ME composites as ME effect is a resistivity-dependent property. Also, this decrease in magnetoelectric voltage coefficient is attributed to the low resistivity of the ferrite phase compared to that of ferroelectric phase, resulting in the leakage of charges developed in the piezoelectric grains through the low-resistance path of the surrounding ferrite grains [42,43].

4. Conclusion

ME composites containing $BaZr_{0.08}Ti_{0.92}O_3$ and $NiFe_{1.9}Mn_{0.1}O_4$ were successfully prepared by standard ceramic method. Cubic spinel ferrite and tetragonal perovskite ferroelectric phase formation was confirmed by X-ray diffraction. The grain size is found to be decreasing with increase of ferrite content. The magnetic parameters like saturation magnetization *Ms*, magnetic moment n_B Bohr magneton and retentivity *Mr* increases as ferrite content increases. The temperature-dependent resistivity reflects the semiconducting behavior of the ME composites. The dielectric dispersion with frequency has been explained on the basis of an electron–hole hopping mechanism which is responsible for conduction and polarization. The measurements of dielectric constant and ac conductivity with frequency suggest that the conduction in composites is similar to the conduction in ferrites and occurs due to polaron hopping. The ME output is found to be decreasing with increase of ferrite content. This phenomenon concludes the effect of grain size on the resistivity of composites which affects the ME effect. The ME output of such composites are useful to fabricate the magnetic field sensors and may also be applicable in many linear ME devices.

Acknowledgments

One of the authors Mr. R.C. Kambale is grateful to the UGC-New Delhi, for providing the financial assistance through UGC - Meritorious research fellowship. This work was carried out under the financial support of UGC-SAP program.

References

[1] H. Schmid, Ferroelectrics 162 (1994) 317.
[2] M. Fiebig, J. Phys. D 38 (2005) R123.
[3] W. Eerenstein, N.D. Mathur, J.F. Scott, Nature (Lond.) 442 (2006) 759.
[4] M.I. Bichurin, Ferroelectrics 204 (1997) 356.
[5] M.I. Bichurin, Ferroelectrics 280 (2002) 385.
[6] M. Fiebig, V.V. Eremenko, I.E.K. Chupis, Proceedings of the MEIPIC-5, Sudak, Ukraine, 2004.
[7] R.E. Newnham, Ferroelectrics 68 (1986) 1.
[8] J.V. Suchetelene, Philips Res. Rep. 27 (1972) 28.
[9] J. Ryu, S. Priya, K. Uchino, H.E. Kim, J. Electroceram. 8 (2002) 107.
[10] L. Mitoseriu, I. Pallecchi, V. Buscaglia, A. Testino, C.E. Ciomaga, A. Stancu, J. Mag. Mag. Mater. 316 (2007) e603.
[11] N. Nanakorn, P. Jalupoom, N. Vaneesorn, A. Thanaboonsombut, Ceram. Int. 34 (2008) 779.
[12] R.A. Islam, D. Viehland, S. Priya, J Mater Sci. 43 (2008) 1497.
[13] J. Ryu, A.V. Carazo, K. Uchino, H.E. Kim, J. Electoceram. 7 (2001) 17.
[14] R.E. Newnham, Rep. Prog. Phys. 52 (1989) 123.
[15] L.G. Van Uitert, J. Chem. Phys. 24 (1956) 306.
[16] J.V.D. Boomgaard, R.A.J. Born, J. Mater. Sci. 13 (1978) 1538.
[17] R.S. Devan, B.K. Chougule, J. Appl. Phys. 101 (2007) 014109.
[18] R.C. Kambale, P.A. Shaikh, S.S. Kamble, Y.D. Kolekar, J. Alloys Compd. 478 (2009) 599.
[19] S.S. Chougule, B.K. Chougule, Smart Mater. Struct. 16 (2007) 493.
[20] D.R. Patil, B.K. Chougule, J. Alloys Compd. 470 (2009) 531.
[21] M.M. Mallapur, M.Phil. Thesis, Shivaji University, Kolhapur, (2003).
[22] J. Smit, H.P.J. Wijn, Ferrites, Cleaver-Human Press, London, 1959.
[23] J. Ryu, S. Priya, K. Uchino, H. Kim, Electroceramics 8 (2002) 107.
[24] C.M. Kanamadi, G. Seeta Rama Raju, H.K. Yang, B.C. Choi, J.H. Jeong, J. Alloys Compd. 479 (2009) 807.
[25] K.K. Patankar, P.D. Dombale, V.L. Mathe, S.A. Patil, R.N. Patil, Mater. Sci. Eng. B 8 (2001) 53.
[26] Y. Zhi, A. Chen, J. Appl. Phys. 91 (2002) 794.
[27] J.C. Maxwell, Electricity, Magnetism, Oxford University Press, London, 1973.
[28] K.W. Wagner, Ann. Phys. 40 (1993) 818.
[29] C.G. Koops, Phys. Rev. 83 (1951) 121.
[30] T.G. Lupeiko, I.B. Lopatina, I.V. Kozyrev, L.A. Derbaremdiker, Inorg. Mater. 28 (1992) 481.
[31] N. Ponpian, P. Balaya, Narayansamy A, J. Phys.: Conden. Mater. 14 (2002) 3221.
[32] B. Vishwanathan, V.R.K. Murthy, Ferrite Materials, Science, Technology, Narosa, New Delhi, 1990.
[33] R.P. Mahajan, K.K. Patankar, M.B. Kothale, S.A. Patil, Bull. Mater. Sci. 23 (4) (2000) 273.
[34] S.A. Lokare, R.S. Devan, B.K. Chougule, J. Alloys Compd. 454 (2008) 471.
[35] R.S. Devan, Y.D. Kolekar, B.K. Chougule, J. Alloys Compd. 461 (2008) 678.
[36] K.K. Patankar, S.S. Joshi, B.K. Chougule, Phys. Lett. A 346 (2005) 337.
[37] D. Adler, J. Feinleib, Phys. Rev. B 2 (1970) 3112.
[38] S.V. Suryanarayana, Bull. Mater. Sci. 17 (7) (1994) 1259.
[39] S. Choudhury, Y.L. Li, C. Krill, L.Q. Chen, Acta Mater. 55 (2007) 1415.
[40] H.M. Duiker, P.L. Beale, Phys. Rev. B 41 (1) (1990) 490.
[41] R.A. Islam, S. Priya, J. Mater. Sci. 43 (2008) 3560.
[42] A. Hanumaian, T. Bhimasankaram, S.V. Suryanarayan, G. Kumar, Bull. Mater. Sci. 17 (1994) 405.
[43] M. Zeng, J.G. Wan, X.P. Jiang, C.W. Nan, J. Appl. Phys. 95 (2004) 8069.